STUDIA UNIVERSITATIS BABEŞ-BOLYAI, CHEMIA, L, 2, 2005

IMPLEMENTATION OF BIVARIATE POPULATION BALANCE EQUATIONS IN CFD CODES FOR MODELLING NANOPARTICLE FORMATION IN TURBULENT FLAMES

ALESSANDRO ZUCCA, DANIELE L. MARCHISIO, ANTONELLO A. BARRESI

Dipartimento di Scienza dei Materiali ed Ingegneria Chimica Politecnico di Torino
Corso Duca degli Abruzzi, 24 10129 Torino – Italy

ABSTRACT. In recent years the problem of studying particle formation and dynamics in turbulent flames has become more and more important, for both environmental and technological reasons. Information on size and morphology of the particulate matter is often required, since these characteristics largely influence the effects of particles on human health and global climate (in the case of soot), and the features of the produced material (in the case of combustion synthesis). The solution of the population balance equation has to be integrated with Computational Fluid Dynamics (CFD), which needs to be employed for the simulation of temperature, composition and velocity fields of the flame. In this work, the recently proposed Direct Quadrature Method of Moments (DQMOM), which allows the solution of the bivariate population balance equation with low additional computational effort, is applied to the study of soot formation in turbulent non-premixed flames. The model takes into account nucleation, molecular growth, oxidation and aggregation of particles; simplified kinetic rates are employed, while velocity and scalar fields are computed by simulations based on the solution of the Reynolds Averaged Navier Stokes (RANS) equations. The bivariate formulation of the DQMOM (in terms of particle volume and surface area) is implemented and compared with the monovariate formulation (in terms of particle volume). Simulation results show that the DQMOM is a suitable tool for the solution of the considered problem both in the monovariate and in the bivariate case, and evidence the importance of a proper treatment of particle fractal dimension to obtain accurate predictions of the morphological properties of soot aggregates.

1. INTRODUCTION

The interest of the scientific community in combustion formed particulate is twofold. On the one hand, in fact, toxicological and environmental studies have focused the attention of the combustion community on the accurate modelling of the formation of carbonaceous nano- and microparticle (soot) in turbulent flames [1]; on the other hand, combustion sintesized nanoparticles are gaining growing importance in a wide range of applications. In the former case, the particulate matter is an undesired by-product, while in the latter case particles constitute a tailored material, with particular features, which is the main product of the process.

In this work, we will focus in particular on the problem of soot formation, which is caused by incomplete oxidation of the species that constitute the fuel, with the production of benzene molecules, which grow to give polycyclic aromatic hydrocarbons (PAH), considered key compounds in the reactions involved in the first stages of the process [2]. Further growth of these high molecular weight compounds leads to the inception of solid particles that in turn grow by surface reaction and aggregate.

The use of Computational Fluid Dynamics (CFD) for studying turbulent combustion is nowadays quite common, and much progress has been done in the last decades for the prediction of flame temperature and composition. Moreover, the capability of predicting a number of pollutants is an important tool in design and optimization of low-emission burners.

In the case of soot formation, the study of gas-phase reactions leading to nucleation of the first solid particles has to be coupled with the study of the evolution of the particle distribution by solving a population balance equation (PBE), which is a balance equation in terms of the distribution of one or more particle state variables, or internal coordinates. When the mixing time scale is large with respect to the characteristic times of the processes affecting the evolution of the population, which strongly depends on flame temperature and composition profiles, the solution of the PBE must be integrated in a CFD code.

The efficient coupling of the population balance with fluid dynamics computation is still the subject of current research. For homogeneous systems with only one internal coordinate, the population balance can be solved by using one of the many available discretization methods [3]. This implies the solution of a large number of equations (20-40) that makes this approach unsuitable for many CFD applications. An alternative approach is the solution of the transport equations of the moments of the size distribution, using a quadrature formula for the closure of unknown terms. Nodes and weights of the quadrature approximation can be evaluated from the moments of the distribution by using a very efficient algorithm [4, 5]. The method has been recently presented in a direct formulation (Direct Quadrature Method of Moments or DQMOM) [6] that allows one to solve the population balance equation with more than one internal coordinate without intolerable increase in the complexity of the algorithm.

In this work the DQMOM has been applied for the solution of the population balance equation for the prediction of soot formation in turbulent flames. A detailed treatment of this method can be found in the next section. The solution of the bivariate population balance equation will be discussed in detail, and the applicability of the method to the problem of soot formation will be assessed. The test case investigated in this work is an ethylene-air turbulent flame (A) studied by Kent and Honnery [7], for which some experimental data are available. In this flame a turbulent jet of ethylene is burned in still air. The use of this fuel, which assures that a relevant amount of soot is formed, is very common in experimental works on soot formation. Once the model has been validated, it will be applied to the study of soot formation in methane/air lean combustion.

2. MATHEMATICAL MODEL

2.1 Computational Fluid Dynamics (CFD)

CFD is based on the solution of the continuity and Navier-Stokes equations. To take into account the highly irregular nature of turbulence, the components of the velocity vector are usually decomposed in the summation of a mean value and fluctuations; therefore, applying Favre averaging (valid for flows with variable density), the continuity, Navier-Stokes and scalar transport equations become respectively:

$$\frac{\partial \overline{\rho}}{\partial t} + \frac{\partial}{\partial x_i}\left(\overline{\rho}\tilde{U}_i\right) = 0\,, \tag{1}$$

$$\frac{\partial}{\partial t}\overline{\rho}\tilde{U}_i + \frac{\partial}{\partial x_i}\overline{\rho}\tilde{U}_i\tilde{U}_j + \frac{\partial}{\partial x_i}\overline{\rho}\widetilde{u_i u_j} = -\frac{\partial \overline{p}}{\partial x_i} + \nu\frac{\partial^2 \overline{\rho}\tilde{U}_i}{\partial x_j \partial x_j}\,, \tag{2}$$

$$\frac{\partial}{\partial t}\bar{\rho}\tilde{\Phi}_\alpha + \frac{\partial}{\partial x_i}\bar{\rho}\tilde{\Phi}_\alpha\tilde{U}_i + \frac{\partial}{\partial x_i}\bar{\rho}\overline{\phi_\alpha u_i} = \left(\Gamma + \Gamma_t\right)\frac{\partial^2\bar{\rho}\tilde{\Phi}_\alpha}{\partial x_i \partial x_i} + \tilde{S}\left(\mathbf{\Phi}\right) \tag{3}$$

where $\bar{\rho}$ and $\bar{p}$ are the mean density and pressure respectively, ν is the kinematic viscosity, $\tilde{U}_i$ is the Favre-averaged value of the *i*-th component of the fluid mean velocity (we are using Einstein's notation, so that repeated indices imply summation), u_i is the same component of the fluctuation of velocity, Φ_α and ϕ_α are the mean and fluctuating concentration of the α-th scalar, Γ is the molecular diffusivity, Γ_t is the turbulent diffusivity $\left(\Gamma_t = \nu_t / Sc_t\right)$, and $\tilde{S}\left(\mathbf{\Phi}\right)$ is the Favre-averaged chemical source term. The third term on the left-hand side of equation (2), the so-called Reynolds stress tensor, is generated by the decomposition and needs to be closed. As far as the solution of this closure problem is concerned, the standard [8], RNG [9] and 'realizable' [10] *k-ε* models are relatively simple approaches based on the eddy-viscosity concept, where the Reynolds stresses are expressed in terms of mean velocity gradients and of the so-called turbulent viscosity ν_t. If the Reynolds Stress Model (RSM) is employed, the problem is closed by solving transport equations for the turbulent stresses [11,12].

The closure of the chemical source term $\tilde{S}\left(\mathbf{\Phi}\right)$ is another major issue in the modelling of turbulent reacting flows. Some of the most widely used modelling approaches are the Eddy dissipation model [13], the Transported Probability Density Function (PDF) method [14], the Presumed PDF method [15,16] and the laminar flamelet model [17]. A complete and detailed description of these methods can be found in the selected references, and in the book by Fox [18]. We will briefly present the beta-PDF approach, that has been employed in the present work for the description of turbulence-chemistry interaction. The global composition of the system is represented via the *mixture fraction*, which is a conservative scalar defined as follows:

$$\xi = \frac{\Phi_\alpha - \Phi_{\alpha,o}}{\Phi_{\alpha,f} - \Phi_{\alpha,o}}, \tag{4}$$

where Φ_α is the concentration of a generic scalar α, and the subscripts *f* and *o* refer to the fuel and the oxidizer stream respectively (and in general to two different inlet streams trough which the reactants are fed separately). It is clear that, according to the definition in (4), the mixture fraction lays within the range [0,1] ($\xi = 1$ for the 'fuel' stream, and $\xi = 0$ for the 'oxidizer' stream). In a turbulent flow, the mixture fraction is of course a fluctuating quantity; its mean value identifies the global composition of the system, while its variance (ξ'^2) is a measure of the extent of mixedness at the molecular level, and is dissipated during the mixing process.

The method requires to solve the transport equations for the mean mixture fraction and the mixture fraction variance:

$$\frac{\partial}{\partial t}\left(\bar{\rho}\tilde{\xi}\right) + \frac{\partial}{\partial x_i}\left(\bar{\rho}\tilde{U}_i\tilde{\xi}\right) = \frac{\partial}{\partial x_i}\left(\frac{\mu_t}{\sigma_t}\frac{\partial\tilde{\xi}}{\partial x_i}\right), \tag{5}$$

$$\frac{\partial}{\partial t}\left(\bar{\rho}\overline{\xi'^2}\right)+\frac{\partial}{\partial x_i}\left(\bar{\rho}\tilde{U}_i\overline{\xi'^2}\right)=\frac{\partial}{\partial x_i}\left(\frac{\mu_t}{Sc_t}\frac{\partial\overline{\xi'^2}}{\partial x_i}\right)+2\frac{\mu_t}{Sc_t}\left(\frac{\partial\tilde{\xi}}{\partial x_i}\right)^2-C_\Phi\bar{\rho}\frac{\tilde{\varepsilon}}{\tilde{k}}\overline{\xi'^2}\,, \tag{6}$$

where the last two terms in (6) are the generation and the dissipation term respectively. The constant C_Φ appearing in the dissipation term is usually set equal to 2.

The temperature and composition fields are calculated evaluating the temperature and composition corresponding to each value of mean mixture fraction $\tilde{\xi}$, mixture fraction variance $\overline{\xi'^2}$, and of enthalpy $\tilde{H}$ for non-adiabatic systems; for non-adiabatic systems, the average value of the scalar Φ_α can be evaluated by the following integral:

$$\tilde{\Phi}_\alpha=\int_0^1 f_\zeta(\xi)\,\Phi_\alpha\left(\xi,\tilde{H}\right)d\xi\,, \tag{7}$$

where $f_\zeta(\xi)$ is the mixture fraction PDF, and $\Phi_\alpha\left(\xi,\tilde{H}\right)$ is the relationship that links mixture fraction, mixture fraction variance and enthalpy to the scalar concentration Φ_α.

Several presumed shapes of PDF have been employed for the mixture fraction, such as the beta-PDF and the double-delta-PDF. By using the beta-PDF approach, the mixture fraction PDF is described as follows [15]:

$$f_\zeta(\xi)=\frac{\xi^{\alpha-1}(1-\xi)^{\beta-1}}{\int_0^1\xi^{\alpha-1}(1-\xi)^{\beta-1}d\xi}\,, \tag{8}$$

where

$$\alpha=\tilde{\xi}\left[\frac{\tilde{\xi}\left(1-\tilde{\xi}\right)}{\overline{\xi'^2}}-1\right], \tag{9}$$

$$\beta=\left(1-\tilde{\xi}\right)\left[\frac{\tilde{\xi}\left(1-\tilde{\xi}\right)}{\overline{\xi'^2}}-1\right]. \tag{10}$$

For a number of possible values of mean mixture fraction and mixture fraction variance, the values of temperature and chemical species involved in the reaction are computed (through Eq. (7)) and stored in a look-up table. In this way the turbulent-chemistry interactions are pre-processed and calculations do not need to be repeated at each iteration, thus resulting in a relevant saving of computational resources.

The treatment of chemistry is hidden in the function $\Phi_\alpha(\xi$ which can be evaluated by different options. An option which is widely used for combustion computations is the *equilibrium assumption*. In this case the equilibrium composition and temperature are evaluated for each value of mixture fraction, variance and enthalpy (if it is the case) by minimization of the Gibbs free energy of the mixture. No detailed kinetic data are required (the reactions are assumed infinitely fast but reversible), and only the species present in the system have to be specified.

Once the mixture fraction PDF is evaluated in the whole domain by solving Eqs. (5) and (6), the temperature and composition profiles are obtained by reading the appropriate value in the look-up table. The mean value of scalars in each computational cell is calculated by interpolation between the neighbouring stored values.

2.2 The Direct Quadrature Method of Moments (DQMOM)

As already stated, the solution of the population balance, which is necessary when the prediction of the evolution of a population of particles is of interest, has to be coupled, in the case of combustion-formed particulate, with the simulation of temperature and composition fields of the flame within a CFD code.

Among the possible solution techniques, we present in this section the DQMOM, which requires low additional computational cost and is therefore suitable for this kind of application.

Let us consider the population balance equation:

$$\frac{\partial \tilde{n}(\boldsymbol{\xi};\mathbf{x},t)}{\partial t}+\frac{\partial}{\partial x_i}\tilde{U}_i\tilde{n}(\boldsymbol{\xi};\mathbf{x},t)-\frac{\partial}{\partial x_i}\left[\Gamma_t\frac{\partial \tilde{n}(\boldsymbol{\xi};\mathbf{x},t)}{\partial x_i}\right]=S(\boldsymbol{\xi};\mathbf{x},t), \tag{11}$$

where $\tilde{n}$ is the Favre averaged number density function, $\boldsymbol{\xi}$ is the internal coordinate vector (i.e., the vector of particle state variables), $\mathbf{x}$ is the spatial coordinate vector, and $S(\boldsymbol{\xi};\mathbf{x},t)$ is the source term, which takes into account continuous and discontinuous changes in the internal coordinates vector, due to, e.g., molecular surface growth, oxidation, aggregation and breakage. The method is based on the moments approach, so that Eq. (11) is solved in terms of the mixed moments of the distribution which, for a generic multivariate number density function, are defined as follows:

$$m_{k_1,k_2,\ldots,k_M}=\int_{-\infty}^{\infty}\xi_1^{k_1}\int_{-\infty}^{\infty}\xi_2^{k_2}\cdots\int_{-\infty}^{\infty}\xi_n^{k_M}\tilde{n}(\boldsymbol{\xi};\mathbf{x},t)\,d\xi_1 d\xi_2\cdots d\xi_M \tag{12}$$

where k_i is the order of the moment with respect to ξ_i.

In this case, the source terms for the moments need to be closed; the main idea behind the approach is the use of a quadrature approximation of the number density function [4, 5]. This corresponds to the approximation of the PSD as follows:

$$\tilde{n}(\boldsymbol{\xi};\mathbf{x},t)\approx\sum_{\alpha=1}^{N}w_\alpha(\mathbf{x},t)\prod_{i=1}^{M}\delta\left[\xi_i-\xi_{i\alpha}(\mathbf{x},t)\right], \tag{13}$$

where $w_\alpha(\mathbf{x},t)$ are the 'weights' and $\xi_{i\alpha}(\mathbf{x},t)$ are the 'abscissas' of the quadrature approximation, M is the number of internal coordinates, and δ indicates the Dirac delta function. Therefore, the mixed moments of the distribution can be written as:

$$m_{k_1,k_2,\ldots,k_M}=\sum_{\alpha=1}^{N}w_\alpha\prod_{i=1}^{M}\xi_{i\alpha}^{k_i}\,. \tag{14}$$

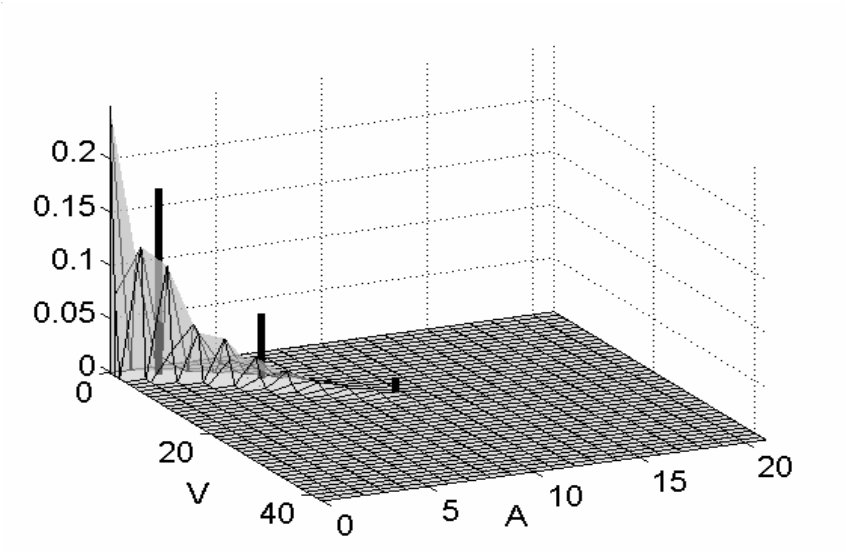

Figure 1. Comparison between a bivariate number density function with respect to surface area and volume (pure coalescence of droplets), and its quadrature approximation with three nodes (black peaks).

It is possible to show that weights and abscissas of the quadrature approximation can be computed forcing them to yield known values of the moments; this can be done either resorting to the Product-Difference (PD) algorithm and solving an eigenvalue-eigenvector problem [19] (but in this case the problem becomes extremely complex when we need to deal with more than one internal coordinate), or directly solving the transport equation of weights and abscissas, as explained by Marchisio and Fox [6]. The DQMOM is based on the latter approach. Let us consider the bivariate case, which has been investigated in the present work: we need to solve the following equations:

$$\frac{\partial w_\alpha}{\partial t} + \frac{\partial}{\partial x_i}\left(\bar{U}_i w_\alpha\right) - \frac{\partial}{\partial x_i}\left[\Gamma_t \frac{\partial w_\alpha}{\partial x_i}\right] = a_\alpha , \tag{15}$$

$$\frac{\partial \varsigma_{1,\alpha}}{\partial t} + \frac{\partial}{\partial x_i}\left(\bar{U}_i \varsigma_{1,\alpha}\right) - \frac{\partial}{\partial x_i}\left[\Gamma_t \frac{\partial \varsigma_{1,\alpha}}{\partial x_i}\right] = b_{1,\alpha} , \tag{16}$$

$$\frac{\partial \varsigma_{2,\alpha}}{\partial t} + \frac{\partial}{\partial x_i}\left(\bar{U}_i \varsigma_{2,\alpha}\right) - \frac{\partial}{\partial x_i}\left[\Gamma_t \frac{\partial \varsigma_{2,\alpha}}{\partial x_i}\right] = b_{2,\alpha} \tag{17}$$

where $\varsigma_{i,\alpha} = w_\alpha \xi_{i,\alpha}$ indicates the α-th 'weighted abscissa', and a_α, and $b_{i,\alpha}$ are the source terms. It is possible to show that such source terms can be easily evaluated solving a linear algebraic system, obtained from the population balance equation after the application of the quadrature approximation and forcing the moments to be tracked with high accuracy [6].In principle, if *N* nodes are employed to follow the evolution of *M*

internal coordinates, the method requires the solution of balance equations for $N(M+1)$ scalars, and therefore the solution of a linear system of correspondent rank. We will focus our attention on the bivariate case, which is of interest in the case of soot formation; in this case the number density function is approximated by the following expression:

$$\tilde{n}\left(\xi_1,\xi_2;\mathbf{x},t\right)=\sum_{\alpha=1}^{N} w_\alpha\left(\mathbf{x},t\right)\cdot\delta\left[\xi_1-\xi_{1,\alpha}\left(\mathbf{x},t\right)\right]\cdot\delta\left[\xi_2-\xi_{2,\alpha}\left(\mathbf{x},t\right)\right] \tag{18}$$

and we need to solve for $3N$ scalars (N weights and $2N$ abscissas). A graphical representation of the bivariate quadrature approximation on which the DQMOM is based is depicted in Fig. 1, where a bivariate number density function and its DQMOM representation are compared. If we substitute Eq. (18) into Eq.(11), and rewrite the population balance in terms of the moments of the distribution, we obtain the following linear system:

$$\sum_{\alpha=1}^{N}\left[\left(1-k-l\right)\xi_{1,\alpha}^{k}\xi_{2,\alpha}^{l}a_\alpha+k\xi_{1,\alpha}^{k-1}\xi_{2,\alpha}^{l}b_{1,\alpha}+l\xi_{1,\alpha}^{k}\xi_{2,\alpha}^{l-1}b_{2,\alpha}\right]=\bar{C}_{k,l}+S_{k,l}^{(N)} \tag{19}$$

where $S_{k,l}^{(N)}$ is quadrature approximation with N nodes of the source term for the mixed moment of order k with respect to the first internal coordinate (the volume V in our case), and of order l with respect to the second internal coordinate (the surface area A), and $\bar{C}_{k,l}$ is a correction term which is needed due to the finite-mode representation of the distribution, and is effective only for moments of order two or higher. It is a function of the gradients of internal coordinates, and is evaluated as follows:

$$\bar{C}_{k,l}=\left(\Gamma+\Gamma_t\right)\sum_{\alpha=1}^{N} w_\alpha\left[k\left(k-1\right)V_\alpha^{k-2}A_\alpha^{l}\frac{\partial V_\alpha}{\partial x_i}\frac{\partial V_\alpha}{\partial x_i}+2klV_\alpha^{k-1}A_\alpha^{l-1}\frac{\partial V_\alpha}{\partial x_i}\frac{\partial A_\alpha}{\partial x_i}+\right.$$
$$\left.+l\left(l-1\right)V_\alpha^{k}A_\alpha^{l-2}\frac{\partial A_\alpha}{\partial x_i}\frac{\partial A_\alpha}{\partial x_i}\right]. \tag{20}$$

Let us consider, for the sake of simplicity, the case of two nodes; we need to track 6 mixed moments of the distribution. If, for example, we choose the following 6 pure integer moments: m_{00}, m_{10}, m_{01}, m_{20}, m_{02}, m_{30}, considering particle volume (V) and surface area (A) as the two internal coordinates, the linear system (19) becomes:

$$\begin{pmatrix} 1 & 1 & 0 & 0 & 0 & 0 \\ 0 & 0 & 1 & 1 & 0 & 0 \\ 0 & 0 & 0 & 0 & 1 & 1 \\ -V_1^2 & -V_2^2 & 2V_1 & 2V_2 & 0 & 0 \\ -A_1^2 & -A_2^2 & 0 & 0 & 2A_1 & 2A_2 \\ -2V_1^3 & -2V_2^3 & 3V_1^2 & 3V_2^2 & 0 & 0 \end{pmatrix}\begin{pmatrix} a_1 \\ a_2 \\ b_{V1} \\ b_{V2} \\ b_{A1} \\ b_{A2} \end{pmatrix}=\begin{pmatrix} \overline{S_{00}}^{(2)} \\ \overline{S_{10}}^{(2)} \\ \overline{S_{01}}^{(2)} \\ \overline{S_{20}}^{(2)}+\overline{C_{20}} \\ \overline{S_{02}}^{(2)}+\overline{C_{02}} \\ \overline{S_{30}}^{(2)}+\overline{C_{30}} \end{pmatrix}, \tag{21}$$

We can evaluate the quadrature approximations of the source terms, $\overline{S}_{k,l}^{(N)}$, as described in the following of this section.

Nucleation

For numerical reasons, it is convenient to assume the nucleation of a uniform distribution of nuclei of volume $0 \le v_0 \le \varepsilon_V$ and surface area $0 \le a_0 \le \varepsilon_A$; in this case we obtain the following expression for the nucleation source term:

$$\bar{S}_{k,l}^{(N)} = J(\mathbf{x},t)\frac{\varepsilon_V^k \varepsilon_A^l}{(k+1)(l+1)}, \tag{22}$$

where $J(\mathbf{x},t)$ is the nucleation rate.

In this way, we can compute by the PD algorithm the values of the distinct abscissas corresponding to the nuclei distribution, and use these values to initialize the DQMOM in the regions where particle number density is null, and the matrix of system (19) would be otherwise singular.

Aggregation

If the result of aggregation is a fractal cluster with fractal dimension D_f, and if we assume the following scaling relationship between surface area and volume:

$$\frac{A}{a_0} = \left(\frac{V}{v_0}\right)^{\frac{2}{D_f}}, \tag{23}$$

where a_0 and v_0 are the area and volume of primary particles, then the source term of moments due to aggregation becomes:

$$\bar{S}_{k,l} = \frac{1}{2}\iiint_0^\infty \left[(V_1+V_2)^k \left(A_\alpha^{\frac{D_f}{2}} + A_\gamma^{\frac{D_f}{2}} \right)^{\frac{2l}{D_f}} - V_1^k A_2^l - V_1^k A_2^l \right] \cdot \tag{24}$$

$$\cdot \beta(V_1,V_2,A_1,A_2)\, n(V_1,A_1)\, n(V_2,A_2)\, dV_1 dV_2 dA_1 dA_2,$$

and, after the application of the quadrature approximation:

$$S_{k,l}^{(N)} = \frac{1}{2}\sum_{\alpha=1}^{N}\sum_{\gamma=1}^{N} \left\{ (V_\alpha + V_\gamma)^k \left(A_\alpha^{\frac{D_f}{2}} + A_\gamma^{\frac{D_f}{2}} \right)^{\frac{2l}{D_f}} - V_\alpha^k A_\alpha^l - V_\gamma^k A_\gamma^l \right\} \beta_{\alpha,\gamma} w_\alpha w_\gamma ; \tag{25}$$

we can observe that the terms in curly brackets represent the contributions (positive) of the aggregate and (negative) of the parent particles to the moment $m_{k,l}$

Molecular growth

When considering continuous changes, in general we can account for the drift term for each coordinate independently. If we denote with $G_V(V,A)$ and $G_A(V,A)$ the rate of continuous change of volume and surface area respectively, the source term of the moments is:

$$\bar{S}_{k,l}^{(N)} = \sum_{\alpha=1}^{N} w_\alpha \left[k V_\alpha^{k-1} A_\alpha^l G_V(V_\alpha, A_\alpha) + l V_\alpha^k A_\alpha^{l-1} G_A(V_\alpha, A_\alpha) \right]. \tag{26}$$

Usually, a variation of volume results in a corresponding variation of surface area according to the appropriate volume/area scaling relationship. On the contrary, a change in surface area can be due not to a net mass flux between the particle and

the environment, but to changes in particle structure, as a consequence of external forces; in this case only the surface area is varied, while volume is not affected by the process ($G_V(V,A)=0$).

2.3 Fractal dimension

When solving the population balance in terms of only one internal coordinate, e.g. particle diameter or volume, (monovariate case) the value of the fractal dimension has to be assumed or evaluated independently. The simplest choice is to fix a unique constant value for all the particles; this is quite a rough approximation, since it is known that aged soot aggregates undergo some restructuring processes that compact the aggregates increasing their fractal dimension [20, 21]. An alternative approach, recently proposed by Artelt *et al.* [22], relates the fractal dimension to the ratio $\tau = t_c / t_r$ of the characteristic collision time $t_c = \left(\bar{\beta} \cdot m_0\right)^{-1}$, where $\bar{\beta}$ is the mean aggregation kernel and m_0 is the number concentration of particles (i.e., the zero-th moment of the distribution), to the characteristic restructuring time t_r. If it is assumed that the restructuring of soot particles is due to an elastic-mechanical strain effect, the characteristic time t_r can be considered equal to a turbulence time micro-scale $\left(t_r = \sqrt{15\nu/\varepsilon}\right)$, so that the rate of the restructuring process is assumed proportional to the shear rate inside the turbulent eddy.

According to Artelt *et al.* [22], the evolution of the fractal dimension can be modelled as:

$$D_f = \begin{cases} D_{f,\min} + \left(D_{f,0} - D_{f,\min}\right)^{1/\tau^s} & \tau \le 1 \\ D_{f,\max} + \left(D_{f,\max} - D_{f,0}\right)^{\tau^s} & \tau > 1 \end{cases} . \tag{27}$$

In Eq.(27), $D_{f,\min} \ge 1$ and $D_{f,\max} \le 3$ are the minimum and maximum value of the fractal dimension, corresponding to the limiting cases for $t_c \ll t_r$ and $t_c \gg t_r$ respectively, $D_{f,0}$ is the fractal dimension at which the characteristic times of the two processes are equal, which is assumed to be the arithmetic average value between the limiting cases, and *s* is a parameter that defines the slope of fractal dimension variation. A detailed discussion of these approaches can be found in [23], where the solution of the monovariate population balance equation was extensively treated. A more rigorous treatment of the fractal properties of aggregates requires the solution of a bivariate population balance equation, which has been implemented and compared with the monovariate simulation in the present work.

2.4 Kinetic models for soot formation

The model takes into account nucleation of particles, molecular growth, aggregation and oxidation of soot particles. Since the main objective of this work is to assess the performance of the bivariate DQMOM for this kind of application, simplified kinetic models were employed, in order to avoid unnecessary CPU load required for the implementation of detailed kinetics. Several models available in the

related literature were tested, and the rate expressions that gave the best agreement with experimental data are reported in Tab. 1. Acetylene is chosen as the key compound for nucleation and molecular growth. The aggregation kernel, which depends on the Knudsen number (the ratio between the mean-free-path of gas molecules, λ, and the particle radius: $Kn = 2\lambda/L$), was evaluated by the Fuchs interpolation formula [27], which is valid in the transition regime between the free molecule ($Kn \ll 1$) and the continuum ($Kn \gg 1$) regime. All the rate expressions were adapted to take into account the fractal dimension D_f of the particle.

The radiative transfer due to soot particles was taken into account by introducing an additional source term for the energy equation:

$$\dot{Q}_{rad} = -\sigma \cdot a_S \cdot \left(T^4 - T_\infty^4\right), \tag{28}$$

where σ is the Stefan-Boltzmann constant, a_S is the soot absorption coefficient, and T_∞ is the radiative environment temperature (set to 300 K).

The absorption coefficient was evaluated by the expression recently proposed by Widmann [28]:

$$a_S = 2370 \cdot T \cdot f_V \tag{29}$$

where f_V is the soot volume fraction.

2.5 Numerical details

Process	Rate expression	Ref.
Nucleation ($m^{-3}s^{-1}$)	$J = N_A \cdot \rho^2 \cdot T^{\frac{1}{2}} \cdot 6 \cdot 10^6 \cdot \exp\left(-\frac{46100}{T}\right) X_{C_2H_2}$	[24]
Molecular Growth ($m\ s^{-1}$)	$G_{mg} = \frac{6}{D_f \rho_s}\left(\frac{R_c}{R_{c0}}\right)^{3-D_f} \cdot 2 \cdot M_s \cdot \exp\left(-\frac{6038}{T}\right)[C_2H_2]$	[25]
Oxidation ($m\ s^{-1}$)	$G_{ox} = -\frac{P}{D_f \rho_s} \cdot T^{-\frac{1}{2}} \cdot 6.5 \cdot \exp\left(-\frac{26500}{T}\right) \cdot Y_{O_2}$	[26]
Aggregation (m^3s^{-1})	$\beta_{12} = 4\pi(D_1 + D_2)(R_{c1} + R_{c2})\left[\frac{R_{c1} + R_{c2}}{R_{c1} + R_{c2} + \left(g_1^2 + g_2^2\right)^{1/2}} + \frac{4(D_1 + D_2)}{(R_{c1} + R_{c2})\left(c_1^2 + c_2^2\right)^{1/2}}\right]^{-1}$ $c_i = \sqrt{\frac{8k_bT}{\pi m_i}} \qquad D_i = \frac{k_bT}{6\pi\mu R_{ci}}\left[\frac{5 + 4Kn_i + 6Kn_i^2 + 18Kn_i^3}{5 - Kn_i + (8+\pi)Kn_i^2}\right] \qquad l_i = \frac{8D_i}{\pi c_i}$ $g_i = \frac{\left(2R_{ci} + l_i\right)^3 - \left(4R_{ci}^2 + l_i^2\right)^{3/2}}{6R_{ci}l_i} - 2R_{ci}$	[27]
Legend	k_b : Boltzmann constant M_S : soot molecular weight N_A : Avogadro's Number X : mole fraction Y : mass fraction	m : particle mass μ .:gas viscosity ρ .:gas density ρ_σ.:soot density

The DQMOM was implemented via user-defined functions within the commercial finite-volume CFD code FLUENT 6.0, which computes the velocity, temperature and composition fields. The standard k-ε model was employed for the turbulence closure, while the mixture-fraction beta-PDF approach with the chemical equilibrium assumption (considering 19 species) was used for modelling micro-mixing and reaction. The particles have been assumed small enough as to have a negligible effect on the global flow-field of the flame, so that the simulation can be monophase. The simulations were carried out with a two-dimensional conformal grid with 10500 rectangular cells.

3. RESULTS AND DISCUSSION

As it has been shown in our work on the solution of the monovariate population balance [23], the agreement with experimental data of temperature and soot volume fraction is quite good for the flame under investigation, even if quite simple modelling approaches have been employed to model turbulence-chemistry interaction and kinetics of soot formation. If we accept the assumption that particle morphology has no effect on the radiative properties of soot and on kinetics of soot formation, the profiles of velocity, temperature and volume fraction shouldn't change passing from the monovariate to the bivariate population balance. The first hypothesis is quite strong, but it is coherent with the model employed for the treatment of radiation, which assumes the absorption effect of soot only proportional to soot volume fraction. The models employed for the kinetics of surface growth and oxidation are instead function of fractal dimension (and therefore particle morphology), but results of the bivariate simulation showed that the profiles of soot volume fractions (reported in Fig. 2) are not significantly different from those obtained in the monovariate case. Therefore, for the bivariate simulations, the velocity, temperature and gas phase composition fields were not updated during the computation, but the profiles computed during monovariate simulations (see [23]) were held constant. In this way, only the transport equations of the six scalars required for the solution of the population balance with the two nodes DQMOM ($w_1, w_2, V_1, V_2, A_1, A_2$) were solved, with significant saving of computational resources.

For the simulations, the choice of only pure moments discussed in the previous section and leading to the linear system in Eq.(21) was implemented. The choice of only pure moments is maybe not the best one, especially if accurate information on the shape of the bivariate particle size distribution is required, since the correlation between internal coordinates is not accounted for properly; however, this choice guarantees both good numerical stability, and good accuracy in the predictions of lower order moments. A more complete discussion of the choice of moments to be tracked, and a validation of the method by comparison with Monte Carlo simulations, can be found in [29].

Aggregation is supposed to lead to particles with the lowest fractal dimension (D_f = 1.8), while the restructuring process is modelled by the following expression, similar to that proposed by Koch and Friedlander [30] for sintering of aggregates formed by primary spherical particles:

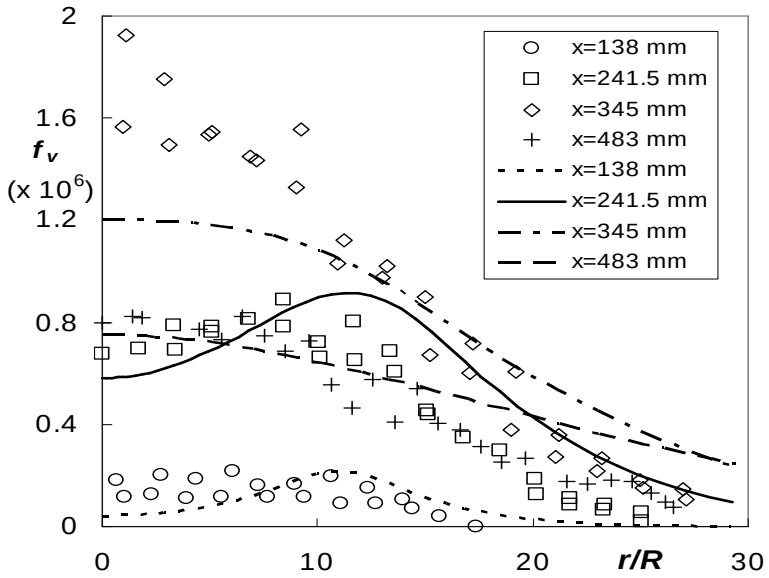

Figure 2. Comparison between experimental (symbols) and simulated (lines) soot volume fraction from bivariate simulations at several heights above the burner.

$$\frac{dA}{dt} = -\frac{1}{t_r}\left(A - A_{\min}\right), \tag{30}$$

where $A_{\min}$ is the surface area of a sphere with the same volume as the restructured particle. The local fractal dimension, which is needed to compute the collision radius and the kinetic expressions for aggregation, oxidation and molecular growth, is computed from the local volume and surface areas through the following equation, derived from Eq. (23):

$$D_f = 2\frac{\ln\left(\frac{V}{v_o}\right)}{\ln\left(\frac{A}{a_0}\right)} \tag{31}$$

The use of a larger number of nodes would result in more accurate predictions, but numerical problems concerning the conditioning of the linear system can hinder convergence.

In Fig. 3 the evolution along the axis of the flame of the fractal dimension (a) and the mean particle size (b) obtained from the bivariate simulation is shown and compared to profiles obtained from the algebraic equation (Artelt's model). As expected, in the first part of the flame aggregation is dominant, and the mean fractal dimension decreases; when, further downstream, aggregation becomes too slow, the restructuring process keeps on increasing fractal dimension and reducing surface area and collision radius. It is possible to see that when Eq. (27) is employed, although the qualitative behaviour is well reproduced, the restructuring rate (and the final fractal

dimension of the aggregates) is overestimated, and the simulated collision radius is lower than in the case of bivariate simulations.

In Fig. 4 the same results reported in Fig. 3 are reported in the area-volume phase plane. In this plot the evolution of the mean particle volume and mean particle surface area (defined as the area of the sphere of radius R_c) is reported. In the same figure, some contour lines at constant fractal dimension are plotted; the trajectories obtained by imposing a constant value of D_f overlap these contour lines. It is clear that the choice of a constant value of fractal dimension is a strong modelling limitation and could represent also a poor approximation if the process under study is characterized by marked morphology changes (as it is for soot formation in turbulent flames).

The agreement between the bivariate and the monovariate simulations is quite good as far as the restructuring rate is not significant, while evident differences are observed in the last part of the flame, where aggregation becomes much less important and the restructuring process makes aggregates more compact, reducing the value of particle surface area.

Even if a validation of the bivariate DQMOM for the prediction of particle morphology still needs to be done, since the bivariate formulation describes with more detail the processes occurring in the flame its prediction will likely be more accurate. However, this study has highlighted the importance of modelling the evolution of particle morphology with the maximum possible detail.

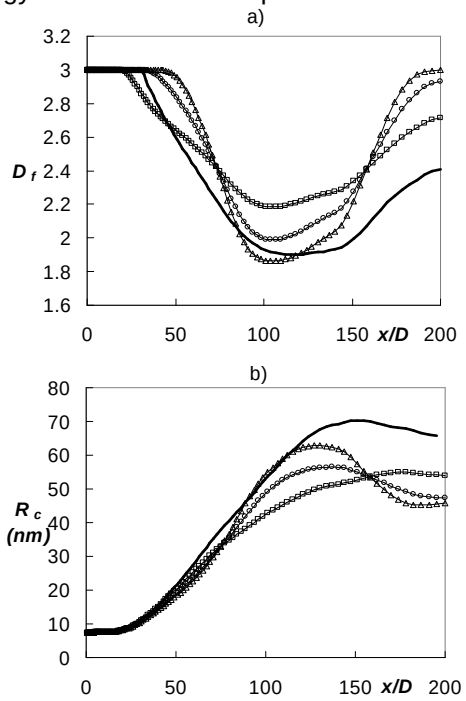

Figure 3: Axial profiles of fractal dimension (a) and collision radius (b). Solid line: bi-variate simulation; symbols: mono-variate simulation with algebraic equation for variation of D_f. Squares: s=0.5; Circles: s=1.0; Triangles: s=1.5.

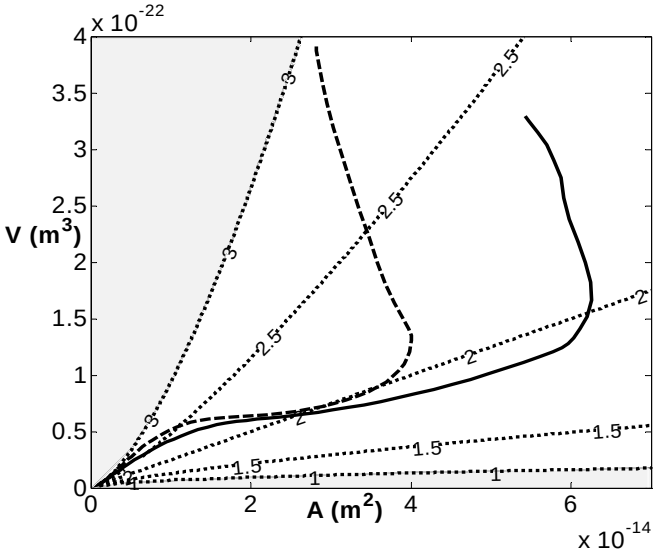

Figure 4. Evolution of particle volume and surface area in the phase plane: comparison between monovariate and bivariate simulations. Dashed line: monovariate simulation (Artelt's model, *s*=1); Dotted lines: contour levels of constant fractal dimension; Solid line: bivariate simulation.

4. CONCLUSIONS

In this work the population balance equation was implemented in a commercial CFD code for modelling soot formation in turbulent diffusion flames. The problem was solved by the DQMOM, which is a novel formulation of the well-known QMOM and presents important advantages for treating multi-variate population balances. Simulation results have shown that the method is a suitable tool for the solution of the considered problem in the mono-variate case, and can be easily extended to the bi-variate case to take into account more rigorously the fractal properties of soot particles.

Acknowledgements

Partial financial support to this research by the Italian Ministry of University and Research (M.I.U.R.) is gratefully acknowledged (PRIN Project 2003: *Combustion formed particulate: mechanisms of formation, low-emission technologies, health and climate effects.*).

Nomenclature

A particle surface area
a source term for weights
a_s absorption coefficient
b source term for abscissas
C correction term

d particle diameter
D_f fractal dimension
f_v soot volume fraction
J nucleation rate
k order of the moments
Kn *K*nudsen number
L abscissa of the quadrature approximation
L *w*eighted abscissa
t time
M n°of internal coordinates
m moment of the distribution
N *n*° of nodes of the quadrature approximation
P pressure
R radius
S source term
T temperature
U mean value of velocity
u fluctuation of velocity
V particle volume
w weight of the quadrature approximation
x spatial coordinate

Greek letters

β aggregation kernel
Γ diffusivity
ε maximum size of nuclei/turbulent dissipation rate
λ mean free path of gas molecules
ν kinematic viscosity
$\boldsymbol{\xi}$ internal coordinate vector
ρ density
σ Stefan-Boltzmann constant
$\boldsymbol{\Phi}$ scalar vector
ϕ fluctuation of scalar concentration

Subscripts

0 primary particle
c coagulation
g gyration
r restructurisation
t turbulent

REFERENCES

1. A. D'Anna, A. Violi, A. D'Alessio, A. F. Sarofim, *Combustion and Flame,* **2001**, *127*, 1995-2003.
2. H. Richter, J. B. Howard, *Progress in Energy and Combustion Science*, **2000**, *26*, 565-608.
3. M. Vanni, *Journal of Colloid and Interface Science,* **2000**, *221*, 143-160.
4. R. McGraw, *Aerosol Science & Technology*, **1997**, *27*, 255-265.
5. D. L. Marchisio, J. T. Pikturna, R. O. Fox, R. D. Vigil, A.A. Barresi, *A.I.Ch.E. Journal*, **2003**, *49*, 1266-1276.

6. D. L. Marchisio, R. O. Fox, *Journal of Aerosol Scence,* **2005**, *36*, 43-73.
7. J. H. Kent, D. Honnery, *Combustion Science and Technology*, **1987**, *54*, 383-397.
8. B. E. Launder, D. B. Spalding, "Lectures in Mathematical Models of Turbulence", Academic Press, London, England, 1972.
9. V. Yakhot, S. A. Orszag, *Journal of Scientific Computing*, **1986**, *1*, 1-51
10. T. H. Shih, W. W. Liou, A. Shabbir, J. Zhu, *Computers and Fluids*, **1995**, *24*, 227-238.
11. B. E. Launder, G. J. Reece, W. Rodi, *Journal of Fluid Mechanics*, **1975**, *68*, 537-566.
12. B. E. Launder, *International Journal of Heat and Fluid Flow*, **1989**, *10*, 282-300.
13. B. F. Magnussen, B. H. Hjertager, *Proceedings of the 16th International Symposium on Combustion*, **1976**, The Combustion Institute, 719-729.
14. S. B. Pope, *Progress in Energy and Combustion Science*, **1985**, *11*, 119-192.
15. J. Baldyga, *Chemical Engineering Science*, **1994**, *49*, 1985-2003.
16. R. O. Fox, *Chemical Engineering and Processing*, **1998**, *37*, 521-535.
17. K. N. Bray, N. Peters, In P. A. Libby and F. A. Williams (eds.), "Chemically Reacting Flows", Academic Press, 1994.
18. R. O. Fox, "Computational models for turbulent reacting flows", Cambridge University Press, Cambridge, UK, 2003.
19. R.G. Gordon, *Journal of Mathematical Physics,* **1968**, *9*, 655.
20. S. Di Stasio, *Journal of Aerosol Science*, **2001**, *32*, 509-524.
21. S. Di Stasio, A.G. Kostandopoulos, M. Kostoglou, *Journal of Colloid and Interface Science*, **2002**, *247*, 33-46.
22. C. Artelt, H. J. Schmid, W. Peukert, *Journal of Aerosol Science*, **2003**, *34*, 511-534.
23. A. Zucca, D. L. Marchisio, A. A. Barresi, R. O. Fox, *Chemical Engineering Science*, **2005**, to appear.
24. J. B. Moss, C. D. Stewart, K. J. Young, *Combustion and Flame*, **1995**, *101*, 491-500.
25. F. Liu, H. Guo, G. J. Smallwood, O. Gulder, *Combustion Theory and Modelling*, **2003**, *7*, 301-315.
26. R. Said, A. Garo, R. Borghi, *Combustion and Flame*, **1997**, *108***,** 71-86.
27. N. A. Fuchs, "Mechanics of Aerosols", Pergamon, New York, U.S.A., 1964.
28. J. F. Widmann, *Combustion Science and Technology,* **2003**,*175*, 2299-2308.
29. A. Zucca, "Modelling of turbulence-chemistry interaction and soot formation in turbulent flames.", Ph.D. Thesis, Politecnico di Torino, Torino, 2005.
30. W. Koch, S. K. Friedlander, *Journal of Colloid and Interface Science,* **1990**, *140*, 419-427.